Electronic Supplementary Information (ESI)

A new surfactant-introduced strategy for separating pure single-phase of metal-organic frameworks

Jun Zhao,[ab] Dongsheng Li,⌫[a] Wenwen Dong,[a] Yapan Wu,[a] Yenan Wang,[a] Bin Liu⌫[c] and Qichun Zhang⌫[b]

[a]College of Materials and Chemical Engineering, Hubei Provincial Collaborative Innovation Center for New Energy Microgrid, China Three Gorges University, Yichang 443002, P. R. China. E-mail: lidongsheng1@126.com.

[b]School of Materials Science and Engineering, & Division of Chemistry and Biological Chemistry, School of Physical and Mathematical Sciences
Nanyang Technological University, Singapore 639798, Singapore. E-mail: qczhang@ntu.edu.sg

[c]Key Laboratory of Synthetic and Natural Functional Molecule Ministry of Education, College of Chemistry and Materials Science, Northwest University, Xi'an 710069, P.R. China. E-mail:liubin@nwu.edu.cn

Table of Contents

S1:Materials and Measurements

All chemicals were commercially available and used without further purification. FT-IR spectra (KBr pellets) were recorded on a Thermo Electron NEXUS 670 FTIR spectrometer. Elemental analyses were performed on a Perkin-Elmer 2400 Series II analyzer. Thermogravimetric (TG) curves were measured on a NETZSCH 449C thermal analyzer with a heating rate of 10 ^{o}C min^{-1} under air atmosphere. Power X-ray diffraction (PXRD) were studied on a Rigaku Ultima IV diffractometer (Cu Kα radiation, λ = 1.5406 Å). Variable-temperature magnetic susceptibility measurements were carried out on a Quantum Design MPMS-XL-7 SQUID magnetometer, and the diamagnetic corrections were evaluated by using Pascal's constants. The simulated powder patterns were calculated using Mercury 2.0. The purity and homogeneity of the bulk products were determined by comparison of the simulated and experimental X-ray powder diffraction patterns.

S2: Experimental Details

Synthesis of two-phase mixture of $[Ni_2(H_2L_2)(bpy)_2]\cdot 2H_2O$ (1) and $Ni_2L(bpy)_{1.5}$(2).A mixture of H_4L (20.3 mg, 0.05 mmol), bipy (7.8 mg, 0.05 mmol), $Ni(NO_3)_2\cdot 6H_2O$ (58.2 mg, 0.2 mmol) and H_2O (5 mL) were placed in a Parr Teflon-lined stainless steel vessel (23 mL) and heated at 160 ^{o}C for 4 days. After the mixture was slowly cooled to room temperature, mixture phase of yellow-green and blue-green crystals were obtained.

Synthesis of $[Ni_2(H_2L_2)(bpy)_2]\cdot 2H_2O$ (1). A mixture of H_4L (20.3 mg, 0.05mmol), bipy (7.8 mg, 0.05 mmol), $Ni(NO_3)_2\cdot 6H_2O$ (58.2 mg, 0.2 mmol), PEG-400 (3 mL) and H_2O (3 mL) were placed in a Parr Teflon-lined stainless steel vessel (23 mL) and heated at 160 ^{o}C for 4 days. After the mixture was slowly cooled to room temperature, pure phase of yellow-green block-shaped crystals were harvested (yield: 82% based on Ni).Anal. Calc. for $C_{62}H_{42}N_6Ni_2O_{18}$: C, 58.34; H, 3.32; N, 6.58 %. Found: C, 58.15; H, 3.10; N, 6.76 %. IR (KBr, cm^{-1}): 3687(s), 3415(s), 3066(m), 2775(s), 2620(s), 2463(m), 1937(m), 1727(s), 1607(s), 1440(s), 1361(s), 1246(s), 1166(s), 1069(s), 804(s), 716(s), 628(s).

Synthesis of $Ni_2L(bpy)_{1.5}$ (2). A similar procedure as 1, except that PEG-400 (3 mL) was replaced by sodium *n*-octanoate (NaC_8) (166.2 mg, 1.0mmol). Pure phase of bright-green cluster-shaped crystals were obtained (yield: 74% based on Ni).Anal. Calc. for $C_{36}H_{21}N_4Ni_2O_8$: C, 57.27; H, 2.80; N, 7.42 %. Found: C, 57.01; H, 2.56; N, 7.61 %. IR (KBr, cm^{-1}): 3048(w), 3060(w), 2460(w), 1634(s), 1544(s), 1445,1383, 1212, 1078, 1015(m), 925(m), 818(s), 701(s), 638(m).

S3: X-ray crystallography study

The diffraction data for compounds **1** and **2** were collected on a RigakuXtaLAB mini diffractometer with graphite monochromated Mo *K*α radiation (λ = 0.71073 Å). The collected data were reduced using the program *CrystalClear*[1]and an empirical absorption correction was applied. The structure was solved by direct methods and refined based on F^2 by the full matrix least-squares methods using SHELXTL.[2,3]Allnon-H atoms were refined anisotropically. The hydrogen atoms of water molecules and carboxylate groups were located from difference Fourier maps and all other hydrogens were included in calculated positions and refined with isotropic thermal parameters riding on those of the parent atoms. The crystallographic data and structural refinement results **1** and **2** are summarized in Table S1, while the selected bond lengths and angles are listed in Table S2.

Table S1 Crystal data and structure refinement details for **1** and **2**.

	1	**2**
Empirical formula	$C_{62}H_{42}Ni_2N_6O_{18}$	$C_{36}H_{21}Ni_2N_4O_8$
Formula weight	1276.44	754.99
Crystal system	$P2_1/n$	*C*mca
space group	Monoclinic	Orthorhombic
a /Å	13.142(6)	31.395(1)
b /Å	12.337(5)	13.702(7)
c /Å	17.656(8)	15.808(8)
α/°	90	90
β /°	108.5(1)	90
γ /°	90	90
V /Å^3	2715(2)	6800(6)
Z	2	8
F(000)	1312	3080
R(int)	0.0789	0.1096
GOF	1.017	1.100
R_1[a)] [I> 2σ(I)]	0.0458	0.0699
wR_2[b)] [I>2σ(I)]	0.1236	0.1984
R_1 (all data)	0.0554	0.0859
wR_2 (all data)	0.1367	0.2111

$\Delta\rho_{max,\ min}$ /e·Å^{-3}	0.754/-0.904	0.989/-0.652

a) $R_1 = \Sigma||F_0|| - |F_c|/\Sigma|F_0|$. b) $wR_2 = \{\Sigma[w(F_0^2 - F_c^2)^2]/ \Sigma[w F_0^2]^2\}^{1/2}$

Table S2 Selected bond lengths [Å] and angles [°] for compound **1** and **2**.

		1	
Ni(1)-O(2)#1	1.992(2)	Ni(1)-O(1)	2.0068(19)
Ni(1)-N(2)	2.015(2)	Ni(1)-O(5)	2.026(2)
Ni(1)-O(6)#1	2.047(2)	Ni(1)-Ni(1)#1	2.6937(12)
O(2)#1-Ni(1)-O(1)	167.19(7)	O(2)#1-Ni(1)-N(2)	97.78(8)
O(1)-Ni(1)-N(2)	94.54(8)	O(2)#1-Ni(1)-O(5)	94.28(8)
O(1)-Ni(1)-O(5)	86.76(8)	N(2)-Ni(1)-O(5)	101.05(8)
O(2)#1-Ni(1)-O(6)#1	86.01(8)	O(1)-Ni(1)-O(6)#1	90.17(8)
N(2)-Ni(1)-O(6)#1	91.60(8)	O(5)-Ni(1)-O(6)#1	167.17(8)
		2	
Ni(1)-O(2)#1	1.997(3)	Ni(1)-O(2)#2	1.997(3)
Ni(1)-O(1)	2.008(3)	Ni(1)-O(1)#3	2.008(3)
Ni(1)-N(3)	2.012(5)	Ni(1)-Ni(1)#2	2.6506(19)
Ni(2)-O(3)#4	2.050(4)	Ni(2)-O(3)#4	2.050(4)
Ni(2)-O(3)	2.050(4)	Ni(2)-N(2)#4	2.059(5)
Ni(2)-N(2)	2.059(5)	Ni(2)-O(4)#4	2.191(5)
Ni(2)-O(4)	2.191(5)		
O(2)#1-Ni(1)-O(2)#2	88.77(19)	O(2)#1-Ni(1)-O(1)	90.46(14)
O(2)#2-Ni(1)-O(1)	168.02(13)	O(2)#2-Ni(1)-O(1)#3	90.46(14)
O(1)-Ni(1)-O(1)#3	87.81(19)	O(2)#1-Ni(1)-N(3)	95.72(13)
O(1)-Ni(1)-N(3)	96.25(13)	O(3)#4-Ni(2)-O(3)	158.1(2)
O(3)#4-Ni(2)-N(2)#4	94.68(17)	O(3)-Ni(2)-N(2)#4	99.90(18)
O(3)-Ni(2)-N(2)	94.68(17)	N(2)#4-Ni(2)-N(2)	96.1(3)
O(3)#4-Ni(2)-O(4)#4	62.13(15)	O(3)-Ni(2)-O(4)#4	101.65(16)
N(2)#4-Ni(2)-O(4)#4	156.64(15)	O(3)-Ni(2)-O(4)#4	101.65(16)
N(2)-Ni(2)-O(4)#4	91.0(2)	O(3)-Ni(2)-O(4)	62.13(15)
N(2)-Ni(2)-O(4)	156.64(15)	O(4)#4-Ni(2)-O(4)	91.1(3)

Symmetry transformations used to generate equivalent atoms: For compound **1**:#1: -x,-y+1,-z; For compound **2**:#1: x,-y+1,-z+1; #2: -x,-y+1,-z+1; #3: -x,y,z; #4: -x+1/2, y, -z+1/2.

Table S3 Hydrogen bond distances(Å) and angles (deg) for **2**

D-H···A	d(H···A)	d(D···A)	∠(DHA)
O3–H3A···N3#1	0.854	2.618	172.10
O9–H9B···O6#2	0.847	2.922	151.05
O9–H9A···O4#2	0.847	2.712	175.33
O7–H7A···O9	0.851	2.633	161.50

Symmetry transformations used to generate equivalent atoms: #1: -x+1, -y, -z; #2: 1x-1/2, y-1/2, -z+1/2.

References

1 Rigaku. CrystalClear version 2.0, Rigaku Corporation, Tokyo, Japan, 2009.

2 G. M. Sheldrick, SHELXS-97, Program for the Solution of Crystal Structures, University of

Göttingen, Germany, 1997.

3 G. M. Sheldrick, SHELXL, Program for the Refinement of Crystal Structures, University of Göttingen, Germany, 1997.

S4: Crystal structures of 1 and 2

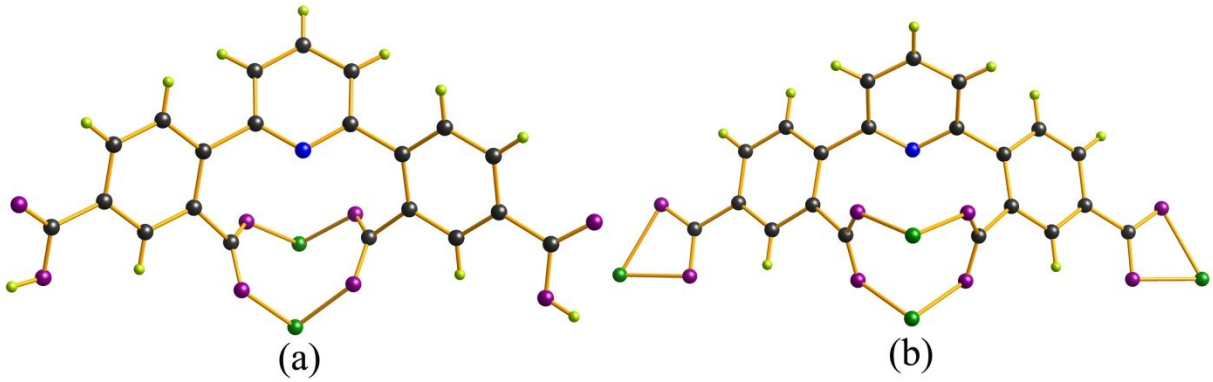

Fig. S1 The two coordination modes of H_4L ligand in **1** (a) and **2** (b).

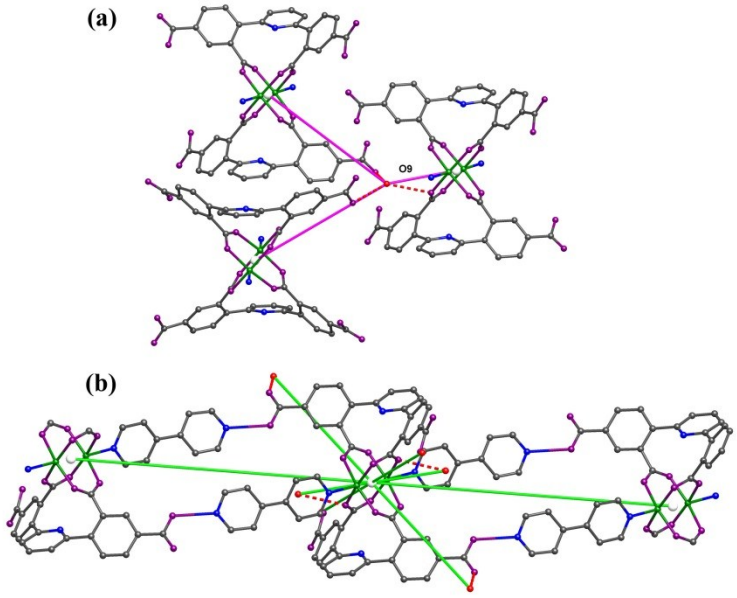

Fig.S2 The schematic representation of 3-connected and 8-connected H-bonded nodes in **1**.

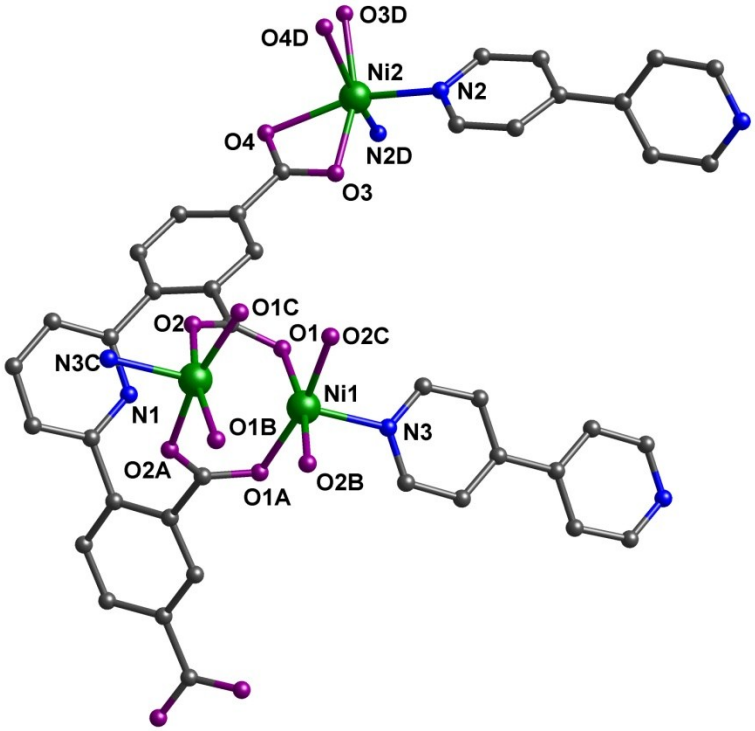

Fig. S3 The coordination environment of Ni(II) atoms of **2** with hydrogen atoms omitted for clarity (A: -x, y, z; B: -x, 1-y, 1-z; C: x, 1-y, 1-z; D: ½-x, y, ½-z).

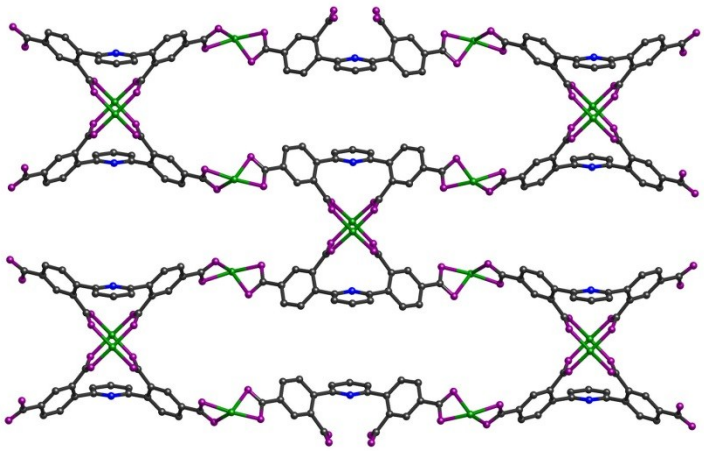

Fig. S4 The 2D sheet constructed by deprotonated L^{4-} ligands and Ni atoms.

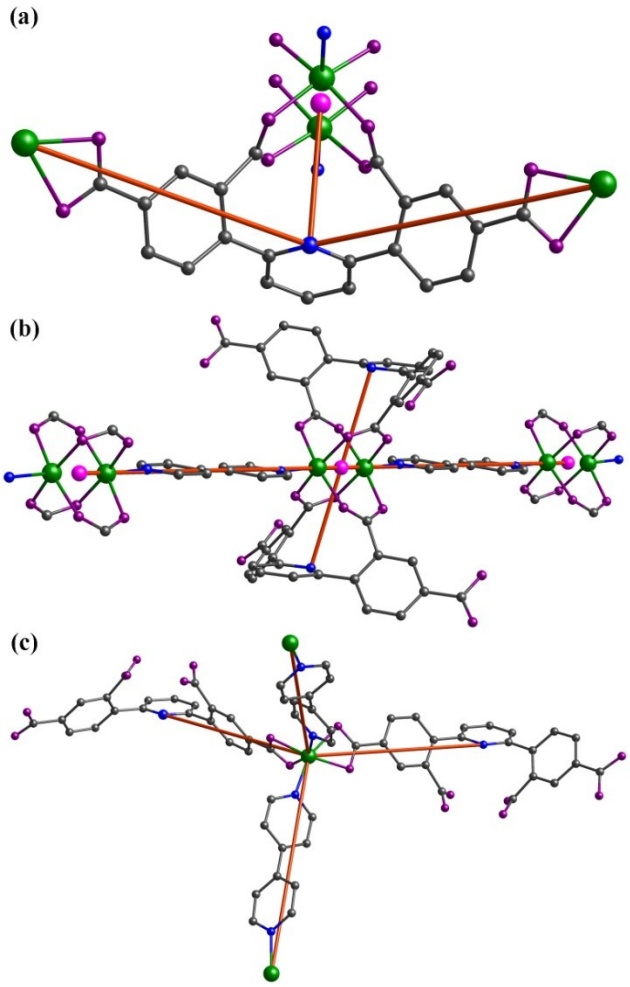

Fig. S5 The schematic representation of (3,4,4)-connected nodes in **2**.

S5: PXRD patterns of the materials

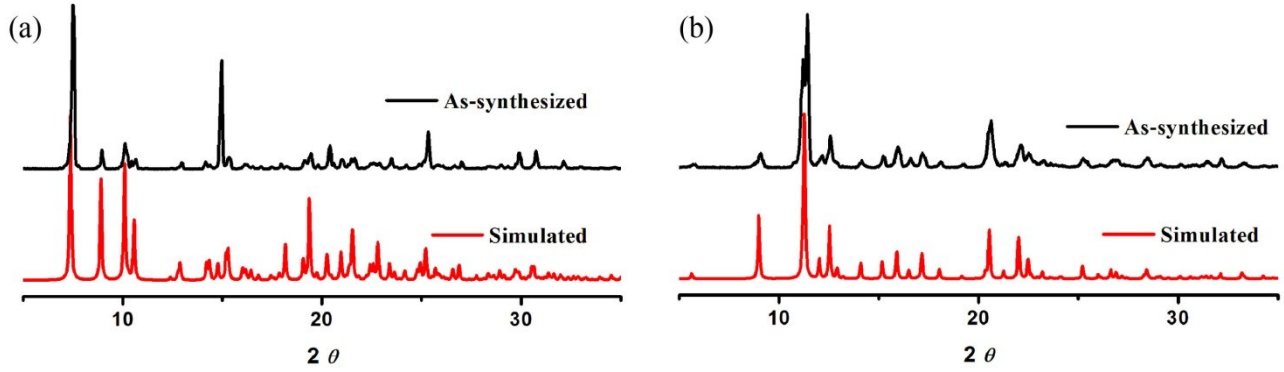

Fig. S6 PXRD patterns for compound **1**and **2** (a for **1**, b for **2**).

S6: TG analyses of the materials

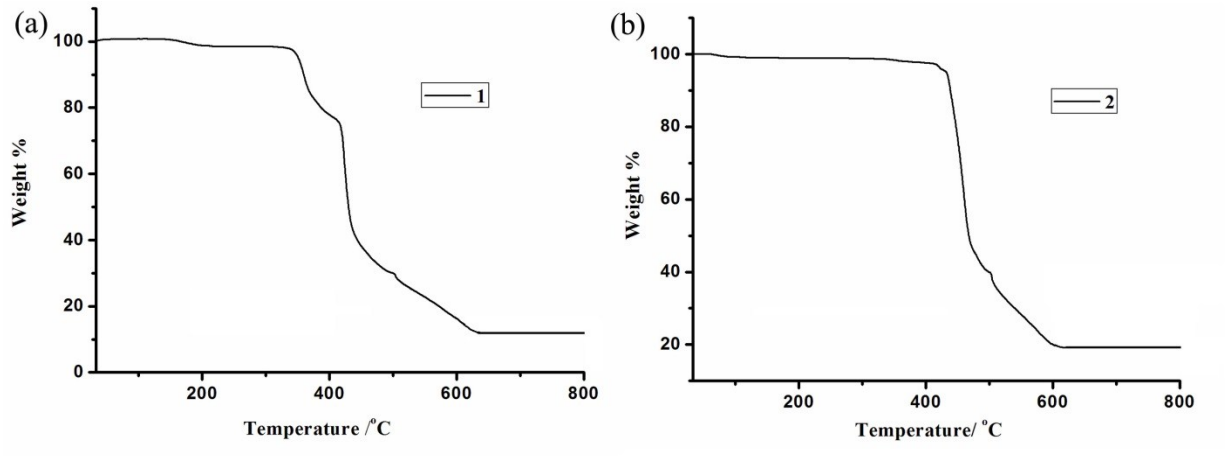

Fig.S7 TGA plots of **1** and **2** under an air environment.

S7: The fitting equations for the magnetic data

The magnetic data of **1** were fitted using the following equation:

$$\chi = (1-\rho)\frac{2Ng^2\beta^2}{kT}\times\frac{e^{2J/kT}+5e^{6J/kT}}{1+3e^{2J/kT}+5e^{6J/kT}}+\frac{4g^2\beta^2}{3kT}\rho \quad (\mathbf{1})$$

$$\chi_M = \frac{\chi}{1-(2zJ/Ng^2\beta^2)\chi} \quad (\mathbf{2})$$

Where J is the exchange interaction and z is the number of nearest neighbors of the metal ion.

For compound **2**, two coupling parameters *J* and *zJ* must be considered to interpret the two possible magnetic interactions in this case. Here, *J* is the exchange couplingparameter in paddlewheel dimer and *zJ* accounts for the rest of interactions. Taking into account the above consideration, the experimental magnetic data can be properly fitted using the following equation, where *N*, *g*, and *k* have their usual meanings. The magnetic data of **2** were fitted using the following equation:

$$\chi = \frac{2Ng^2\beta^2}{kT}\times\frac{e^{2J/kT}+5e^{6J/kT}}{1+3e^{2J/kT}+5e^{6J/kT}}+\frac{4Ng^2\beta^2}{3kT} \quad (\mathbf{3})$$

The presence of weak intermolecular interactions was also considered in the molecular field approximation as equation (**2**).